Filtering-based endmember estimation from snapshot spectral images

Kinan Abbas, Matthieu Puigt, Gilles Delmaire, Gilles Roussel

Filtering-based endmember estimation from snapshot spectral images

Kinan Abbas, Matthieu Puigt, Gilles Delmaire, and Gilles Roussel
Univ. Littoral Côte d'Opale, LISIC – UR 4491, F-62219 Longuenesse, France

***Abstract*— We propose a new endmember estimation method for snapshot spectral imaging (SSI) systems using Fabry-Perot filters. Indeed, such systems only provide a part of the spectral content of a classical multispectral camera and restoring the full datacube from an SSI matrix is named "demosaicing". However, we recently found that a joint unmixing and demosaicing method allowed a much better unmixing performance than a two-stage approach consisting of a demosaicing step followed by an unmixing one. In this paper, we propose a new approach to estimate endmembers from the SSI image without requiring a demosaicing step. It inverts the Fabry-Perot filters and extends the "pure pixel" framework to the SSI sensor patch level. Our proposed scheme is found to significantly outperform SotA methods.**

1 Introduction

Recent technological advances in design and processing speed have successfully demonstrated a new snapshot mosaic imaging sensor architecture (SSI), allowing miniaturized platforms to efficiently acquire the spatio-spectral content of the dynamic scenes from a single exposure. However, SSI systems have a fundamental trade-off between spatial and spectral resolution because they associate each pixel with a specific spectral band. Therefore a post-processing technique known as "demosaicing" must be applied to estimate the full HS data cube. Once the 3-D HS image has been restored from the 2-D SSI one, we can apply any postprocessing technique of interest. In particular, extracting the spectral signatures of all the materials—aka endmembers—which are present in an observed scene is a very classical problem known as *unmixing*. The filters used in SSI systems introduce additional harmonics around each wavelength of interest in real implementation.Thus, the process of endmember extraction and unmixing is complex.

In this work, we propose a novel approach to estimate endmembers from the SSI image by inverting the Fabry-Perot filters to recover the spectral content from "patches" of the SSI image. Then, we relax the abundance sparsity assumption needed in [1]: we here assume that the previously recovered spectra may be seen as linear mixtures of the endmembers and that some of the patches only contained one material, i.e., we extend the "pure pixel" idea to the patch level. The VCA algorithm is then used to derive the final endmembers, while the abundances can then be estimated using the method in [1][1].

2 Problem Statement

The SSI camera acquires a two-dimensional image of $m \times n$ pixels for each exposure, where m and n are the numbers of horizontal and vertical pixels, respectively. Moreover, the camera is assumed to observe k spectral bands. In practice, the considered SSI technology is based on a mosaic of FPfs which consist of $\sqrt{k} \times \sqrt{k}$ patches which are repeated along the sensor surface[2]. In the ideal scenario, an FPf allows the light from a minimal spectral range to propagate to a sensor and stops the light outside this range. However, these filters present additional harmonics around each wavelength of interest in the real implementation. Fortunately, these filters are known and provided by the camera manufacturer [2]. In the remainder of this section, we focus on a single patch of FPfs. Denoting $y_i(\lambda_i)$ the i-th SSI pixel of the considered patch—assumed to theoretically observe the spectral information at λ_i nm—we get:

$$y_i(\lambda_i) = \sum_{j=1}^{k} h_i(\lambda_j) \cdot x_i(\lambda_j) + \omega_i, \tag{1}$$

where $h_i(\lambda)$ is the FPf associated with Pixel i, $x_i(\lambda)$ is the plain spectrum to be observed on Pixel i, and ω_i is some additive noise. Moreover, assuming a linear mixture model, the observed spectrum $x_i(\lambda)$ can be written as

$$x_i(\lambda) = \sum_{l=1}^{p} g_{il} f_l(\lambda), \tag{2}$$

where p is the number of endmembers present in the observed scene, $f_l(\lambda)$ denotes the l-th endmember, and g_{il} its associated abundance proportion in Pixel i where the sum of the abundances equals to one. In this paper, we aim to estimate the p endmembers $f_l(\lambda)$ from the SSI image using Eqs. (1) and (2).

3 Proposed Method

We now introduce our proposed method. First of all, let us emphasize the fact that inverting the k FPfs $h_i(\lambda)$ in Eq. (1) is ill-posed. In order to estimate the endmembers, we need to add additional assumptions. We first assume that in some patches, the matrix X which is defined over the considered patch as

$$X \triangleq \begin{bmatrix} x_1(\lambda_1) & \dots & x_1(\lambda_k) \\ \vdots & & \vdots \\ x_k(\lambda_1) & \dots & x_k(\lambda_k) \end{bmatrix} \tag{3}$$

is approximately rank-1, i.e., $\forall j = 1, \dots, k$, for any given indices i_0 and i_1, $x_{i_0}(\lambda_j) \approx x_{i_1}(\lambda_j)$. Such an assumption is valid for miniaturized SSI systems which can be quite close to the area they tend to observe. For the sake of readability, we drop the indices and reduce the matrix X to a single vector $\underline{x} = [x(\lambda_1), \dots, x(\lambda_k)]$. Denoting ^{T} the transposition,

$$\underline{y} \triangleq [y_1(\lambda_1), \dots, y_k(\lambda_k)]^T, \tag{4}$$

[1] This is why we only focus on the endmember estimation in this paper.

[2] Typical values of k are 16 or 25, such that the patch is of size 4×4 or 5×5, respectively. Moreover, m and n are both proportional to $\sqrt{k}$.

the vector of the k observed pixels in a patch, $\underline{\omega} \triangleq [\omega_1, \ldots, \omega_k]^T$ the associated vector of additive noise, and

$$H \triangleq \begin{bmatrix} h_1(\lambda_1) & \ldots & h_1(\lambda_k) \\ \vdots & & \vdots \\ h_k(\lambda_1) & \ldots & h_k(\lambda_k) \end{bmatrix} \quad (5)$$

the matrix of FPfs, we get

$$\underline{y} = H \cdot \underline{x}^T + \underline{\omega}. \quad (6)$$

Our approach thus reads as follows. For each patch, we first aim to recover a tentative spectrum $\underline{x}$ from Eq. (6). In practice, as the matrix H can be ill-conditionned[3], we aim to solve a penalized optimization problem, i.e.,

$$\min_{\underline{x} \geq 0} \frac{1}{2} \|\underline{y} - H \cdot \underline{x}^T\|_2^2 + \frac{\alpha}{2} \|D \cdot \underline{x}^T\|_2^2, \quad (7)$$

where D is the square matrix accounting for the discrete derivative of the spectrum $\underline{x}$, and α stands for the penalization term. In practice, the error value $\|\underline{y} - H \cdot \underline{\hat{x}}\|_2$—where $\underline{\hat{x}}$ is the estimated spectrum obtained from Eq. (7)—provides a measure of rank-one approximation. Indeed, if in Eq. (6) the content of X cannot be approximated by a single vector, then $\|\underline{y} - H \cdot \underline{\hat{x}}\|_2$ will be high. On the contrary, it will be low if the rank-one approximation is a valid assumption. By only keeping the estimated vectors linked with the lowest errors—say q vectors—we get a $q \times k$ data matrix $\mathbb{X}$ where the FPf effects are removed. Let us recall that these q vectors are associated with q patches which are approximately rank-1. In practice, such a situation may be met if (i) only one endmember is active over the patch, or (ii) the abundance proportions are constant over the patch. The first scenario may be seen as a patch extension of the "pure pixel assumption" [4]—that we call "pure patch assumption"—while the second means that several endmembers are present in similar proportions over the patch.

Denoting G and F the $q \times k$ and $k \times k$ matrices of abundances and endmembers associated with the q rank-1 patches, we get a simple linear mixing relationship

$$\mathbb{X} \approx G \cdot F. \quad (8)$$

In this paper, we further assume that at least one pure patch exists for each endmember to estimate. This means that Eq. (8) can be solved by any unmixing method using the pure patch assumption. In this paper, in order to show the proof of concept, we use VCA [5] and we name our proposed method FPVCA for Filter Patch-based VCA. At this stage, let us stress again that due to the fact that a miniaturized SSI camera may be placed very close to an area to observe, the rank-1 and the pure patch assumptions are not very constraining.

4 Experiments and Conclusion

We compare the performance achieved by our proposed FPVCA method with our previously proposed KPWNMF approach [1] and five 2-step demosaicing-then-unmixing methods. For the latter, we consider five state-of-the-art demosaicing methods—i.e., GRMR [3], BTES [6], WB [7], PPID [8], and ItSD [9]—while in the second step, we extract the endmembers in the restored datacube using the VCA algorithm.

[3]For example, the 5×5 filter matrix H using real FPfs in [3] has two rows which are almost null.

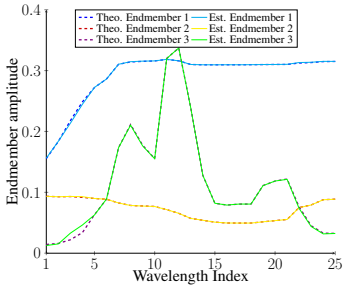

Figure 1: The estimated spectra in case of real filter with patch size 5×5.

Table 1: Average SIR and MRSA (into brackets) values for the considered experiment. In bold: the best values.

	4 x 4 patch		5 x 5 patch	
	Ideal Filter	**Real Filter**	**Ideal Filter**	**Real Filter**
GMRM + VCA	61.6 (4.0)	56.7 (4.8)	10.2 (4.0)	11.5 (3.6)
BTES + VCA	58.2 (4.4)	55.5 (4.9)	9.5 (4.4)	9.7 (4.5)
WB + VCA	61.4 (3.8)	57.7 (4.9)	11.7 (3.8)	12.2 (3.9)
PPID + VCA	73.1 (2.3)	63 (3.7)	28 (2.3)	16.3 (4.2)
ItSD + VCA	61.2 (4.8)	58.6 (4.6)	14.6 (4.8)	14.8 (4.8)
KPWNMF	77.8 (2.2)	64.3 (4.8)	31.8 (2.2)	19.2 (4.0)
FPVCA	**253.0 (0)**	**253.0 (0.0)**	**246.0 (0.0)**	**67.4 (0.8)**

As a consequence, all the considered methods should take advantage of the presence of pure pixels.

To assess the performance of the tested methods, we compare the quality of the restored spectra using the Signal-to-Interference Ratio (SIR, reported in dB) and Mean-Removed Spectral Angle (MRSA) computed over the rows of F. The MRSA measures how close two endmembers are (neglecting scaling and translation) [10]. We first found that a small value of α (typically, $0.001 \leq \alpha \leq 0.02$) allows a much lower MRSA than no regularization ($\alpha = 0$) or than higher values of α. In the remainder of the tests, we set this parameter to $\alpha = 0.005$. Table 1 provides the average SIR and MRSA of the estimated spectra achieved by the various methods in noiseless mixtures. This table shows that the unmixing performance obtained with our proposed FPVCA method is always much better than the other methods. This is probably because all the tested 2-stages approaches introduce some datacube estimation errors that affect the quality of the estimated spectra. Moreover, the performance of our previously proposed KPWNMF approach is slightly better than the SotA other methods but still much lower than FPVCA. This may be due to the fact that the abundance sparsity assumption in [1]—i.e., all the rank-one patches are pure patches—is not necessarily satisfied in these simulations. Still, KPWNMF assumes all the vectors in $\mathbb{X}$ to be close to the true endmembers and estimates the latter using K-means. Such a clustering algorithm may be affected by the spectra obtained from non-pure patches, which lowers its performance.

Please also note the drop of SIR in the case of 5×5 real filters. While our proposed FPVCA approach still outperforms the other methods, its performance decrease is due to the fact that H is severely ill-conditioned. The Tikhonov regularization serves to correct the effect of the matrix H. Furthermore, the angle between the estimated spectra and the real one is small, and they tend to be almost identical, as shown in Fig. 1.

In this paper, we proposed a new method for estimating endmembers from SSI images. It works on an SSI patch level and it mainly consists of finding rank-one patches and of restoring the spectral content from the latter. Then, any unmixing method assuming pure pixels—e.g., VCA—can be applied to the collected data. The proposed method significantly outperforms all the tested 2-stage approaches but also our previous method [1].

References

[1] K. Abbas, M. Puigt, G. Delmaire, and G. Roussel, "Méthode de démélange et dématriçage conjoints fondée sur la complétion de rang un pour les images multispectrales "snapshot"," in *Actes du GRETSI*, (Nancy, France), Sept. 2022.

[2] B. Geelen, C. Blanch, P. Gonzalez, N. Tack, and A. Lambrechts, "A tiny VIS-NIR snapshot multispectral camera," in *Advanced Fabrication Technologies for Micro/Nano Optics and Photonics VIII* (G. von Freymann, W. V. Schoenfeld, R. C. Rumpf, and H. Helvajian, eds.), SPIE, Mar. 2015.

[3] G. Tsagkatakis, M. Bloemen, B. Geelen, M. Jayapala, and P. Tsakalides, "Graph and rank regularized matrix recovery for snapshot spectral image demosaicing," *IEEE Trans. Comput. Imaging*, vol. 5, pp. 301–316, June 2019.

[4] J. M. Bioucas-Dias, A. Plaza, N. Dobigeon, M. Parente, Q. Du, P. Gader, and J. Chanussot, "Hyperspectral unmixing overview: Geometrical, statistical, and sparse regression-based approaches," *IEEE J. Sel. Topics Appl. Earth Observ. Remote Sens.*, vol. 5, pp. 354–379, Apr. 2012.

[5] J. M. P. Nascimento and J. M. Bioucas-Dias, "Vertex component analysis: a fast algorithm to unmix hyperspectral data," *IEEE Transactions on Geoscience and Remote Sensing*, vol. 43, no. 4, pp. 898–910, 2005.

[6] L. Miao, H. Qi, R. Ramanath, and W. Snyder, "Binary tree-based generic demosaicking algorithm for multispectral filter arrays," *IEEE Trans. Image Process.*, vol. 15, pp. 3550–3558, Nov. 2006.

[7] J. Brauers and T. Aach, "A color filter array based multispectral camera," in *12. Workshop Farbbildverarbeitung* (G. C. Group, ed.), (Ilmenau), October 5-6 2006.

[8] S. Mihoubi, O. Losson, B. Mathon, and L. Macaire, "Multispectral demosaicing using pseudo-panchromatic image," *IEEE Trans. Comput. Imaging*, vol. 3, pp. 982–995, Dec. 2017.

[9] J. Mizutani, S. S. Ogawa, K. Shinoda, M. Hasegawa, and S. Kato, "Multispectral demosaicking algorithm based on inter-channel correlation," in *Proc. IEEE VCIP'14*, pp. 474–477, 2014.

[10] N. Gillis and S. A. Vavasis, "Semidefinite programming based preconditioning for more robust near-separable nonnegative matrix factorization," *SIAM Journal on Optimization*, vol. 25, pp. 677–698, jan 2015.